Molecular Cancer Therapeutics

Antibody Format and Drug Release Rate Determine the Therapeutic Activity of Noninternalizing Antibody–Drug Conjugates

Rémy Gébleux[1], Sarah Wulhfard[2], Giulio Casi[2], and Dario Neri[1]

Abstract

The development of antibody–drug conjugates (ADC), a promising class of anticancer agents, has traditionally relied on the use of antibodies capable of selective internalization in tumor cells. We have recently shown that also noninternalizing antibodies, coupled to cytotoxic drugs by means of disulfide linkers that can be cleaved in the tumor extracellular environment, can display a potent therapeutic activity. Here, we have compared the tumor-targeting properties, drug release rates, and therapeutic performance of two ADCs, based on the maytansinoid DM1 thiol drug and on the F8 antibody, directed against the alternatively spliced Extra Domain A (EDA) domain of fibronectin. The antibody was used in IgG or in small immune protein (SIP) format. In both cases, DM1 was coupled to unpaired cysteine residues, resulting in a drug-antibody ratio of 2. In biodistribution studies, SIP(F8)-SS-DM1 accumulated in the tumor and cleared from circulation more rapidly than IgG(F8)-SS-DM1. However, the ADC based on the IgG format exhibited a higher tumor uptake at later time points (e.g., 33%IA/g against 8%IA/g at 24 hours after intravenous administration). In mouse plasma, surprisingly, the ADC products in IgG format were substantially more stable compared with the SIP format (half-lives >48 hours and <3 hours at 37°C, respectively), revealing a novel mechanism for the control of disulfide-based drug release rates. Therapy experiments in immunocompetent mice bearing murine F9 tumors revealed that SIP(F8)-SS-DM1 was more efficacious than IgG(F8)-SS-DM1 when the two products were compared either in an equimolar basis or at equal milligram doses. *Mol Cancer Ther; 14(11); 2606–12. ©2015 AACR.*

Introduction

Conventional cytotoxic agents used for the pharmacotherapy of cancer do not selectively localize at the tumor site, a limitation that contributes to undesired side effects and toxicity to normal organs (1–4). There has been a growing interest in the use of monoclonal antibodies as vehicles for the pharmacodelivery of potent cytotoxic drugs to neoplastic lesions (5–8) with the aim to generate targeted biopharmaceutical agents with improved activity and selectivity. Two antibody–drug conjugates (ADC) are currently approved for clinical applications. Adcetris is composed of the chimeric anti-CD30 antibody cAC10, conjugated to monomethyl auristatin E, through a protease-labile valine-citrulline–containing linker. The product was approved for Hodgkin lymphoma and for systemic anaplastic large cell lymphoma (ALCL) on the basis of objective response rates of a phase II trial (9). Kadcyla consists of the anti-Her2 antibody trastuzumab linked at lysine residues with the maytansinoid derivative DM1, using a noncleavable maleimide-based linker. It has been approved for the treatment of HER2-positive metastatic breast cancer that had previously been treated with Herceptin (trastuzumab) and a taxane (10). In addition, more than 40 products are currently being tested in clinical trials (11).

While it has been claimed that "targeting an ADC to a noninternalizing target antigen with the expectation that extracellularly released drug will diffuse into the target cell is not a recipe for a successful ADC" (12), several lines of evidence indicate that efficacious ADC products can be produced against targets that do not internalize into tumor cells, provided that suitable linker–payload combinations are used. For example, in a systematic study aimed at identifying the optimal targets and linker–drug combinations for the treatment of non-Hodgkin lymphoma, it was found that ADCs with cleavable or hydrolysable linkers (e.g., disulfides, hydrazones) were efficacious even with antibodies specific to targets that were poorly internalized (e.g., CD20, CD21, and CD72). These results suggested that the drug could be released extracellularly, thus permeating the tumor cells after the ADC product had localized on its target (13). These initial findings were strengthened by the observation that ADCs based on disulfide linkers and directed against the alternatively spliced EDA domain of fibronectin, a component of the tumor subendothelial extracellular matrix, can mediate a potent anticancer activity in the mouse. It has been postulated that disulfide-based ADC products may release their payload upon tumor cell death, in a process that can be amplified by the diffusion of the cleaved cytotoxic drug into neighboring cells and by the subsequent release of reducing agents (e.g., cysteine, glutathione; refs. 14–17).

[1]Institute of Pharmaceutical Sciences, Department of Chemistry and Applied Biosciences, ETH Zürich, Zurich, Switzerland. [2]Philochem AG, Otelfingen, Switzerland.

Note: Supplementary data for this article are available at Molecular Cancer Therapeutics Online (http://mct.aacrjournals.org/).

Corresponding Author: Dario Neri, Swiss Federal Institute of Technology, Vladimir-Prelog-Weg 1-5/10, Zurich 8093, Switzerland. Phone: 41-44-6337401; Fax: 41-44-6331358; E-mail: neri@pharma.ethz.ch

doi: 10.1158/1535-7163.MCT-15-0480

In previous therapy experiments, the F8 antibody, specific to the EDA domain of fibronectin (17, 18), was used in small immune protein (SIP) format, consisting of an scFv fragment fused to the εCH4 domain of human IgE. The SIP format contains unpaired C-terminal cysteine residues, which can be reduced and selectively modified without loss of protein stability and antibody activity, yielding site-specific conjugates (15). Conjugation at hinge cysteines typically results in heterogeneous mixtures of products, unless all moieties are modified to achieve a drug-to-antibody ratio of 8 (19, 20). However, the mutation of heavy chain hinge cysteine residues into serines has previously been used for the preparation of chemically defined thioether-based ADCs, with drugs attached at the C-terminal cysteine residue of the light chain (21).

In this work, we have compared two chemically defined ADC preparations of the F8 antibody, using the potent maytansinoid DM1-SH thiol drug as disulfide-linked payload (Fig. 1A). The antibody was used in SIP format and in a mutant IgG format, allowing a site-specific drug coupling at the C-terminal cysteine residue of the light chain. Both SIP(F8)-SS-DM1 and IgG(F8)-SS-DM1 were characterized by quantitative biodistribution analysis and in therapy experiments performed in F9 tumor–bearing mice. Surprisingly, SIP(F8)-SS-DM1 exhibited a more potent anticancer activity, compared with the IgG counterpart, in spite of a lower accumulation at the tumor site at late time points (i.e., 24 hours and beyond). The potent therapeutic activity of SIP(F8)-SS-DM1 can be related to the tumor uptake at early time points (e.g., 3 hours after injection), which was as efficient as the one observed for the IgG format, and to the fact that the SIP-based ADC releases the cytotoxic drug more rapidly (>20-fold) than the corresponding IgG product.

Materials and Methods

Cell culture: cell lines, incubation, and manipulation conditions

Transfected CHO-S cells (Invitrogen) were cultured in suspension in PowerCHO-2CD medium (Lonza), supplemented with

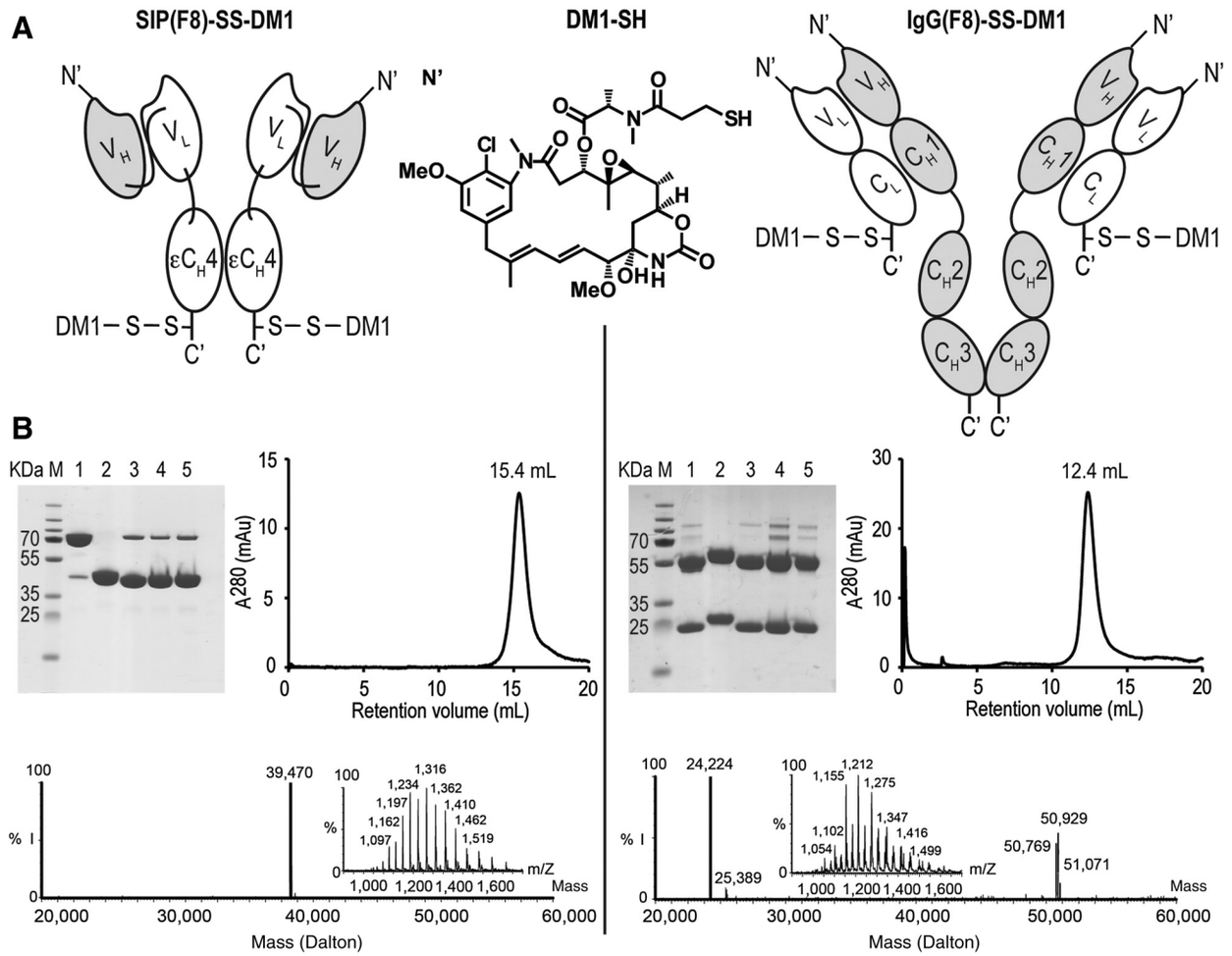

Figure 1.
Characterization of SIP(F8)-SS-DM1 and IgG(F8)-SS-DM1. A, schematic representation of SIP(F8)-SS-DM1, IgG(F8)-SS-DM1, and of the DM1-SH drug. B, biochemical characterization of the products and of reaction intermediates by SDS-PAGE, size-exclusion chromatography, and ESI-MS. The calculated masses of SIP(F8)-SS-DM1 and IgG(F8)-SS-DM1 are 39,464 and 24,218 Daltons, respectively. M, molecular weight marker. Lanes 1 and 2 represent unmodified antibody in nonreducing and reducing conditions, lane 3 the iodoacetamide conjugate, lane 4 the Ellman intermediate, and lane 5 the final DM1 conjugate (% I = % of MS signal intensity).

Ultraglutamine-1 (Lonza), HT-supplement (Gibco), and Antibiotic-Antimycotic (Gibco). F9 murine teratocarcinoma cells (ATCC; CRL-1720) were grown in 0.1% gelatin-coated tissue flasks in DMEM (Gibco) supplemented with 10% FBS (Gibco) and incubated at 37°C in 5% CO_2 atmosphere. The authors did not perform authentication on this cell line.

Animals and tumor models

Ten- to 12-week-old female Sv129Ev mice were obtained from Charles River Laboratories (Germany). F9 teratocarcinoma cells (3.0×10^7) were implanted subcutaneously in the shaved flank. Animals were sacrificed when tumor volumes reached a maximum of 2,000 mm^3 or weight loss exceeded 15%. Experiments were performed under a project license issued by the Veterinäramt des Kantons Zürich, Switzerland (Bew. Nr. 42/2012).

Cloning, expression, and protein characterization

The gene structure for SIP(F8), its cloning, expression, and characterization have previously been described (18). The F8 antibody in IgG format was cloned and expressed in CHO-S cells (Invitrogen) using a previously described strategy (22), except for the cysteine residues of the heavy chain in positions 220, 226, and 229, which were mutated into serine residues. The full aminoacid sequences for SIP(F8) and IgG(F8) can be found in Supplementary Fig. S1.

Antibody–DM1 conjugates preparation

The conjugation of thiol-containing drugs to C-terminal cysteine residues of recombinant antibodies has previously been described (15, 17, 23). Briefly, the antibody in SIP or IgG format was reduced with 30 equivalents of tris(2-carboxyethyl)phosphine hydrochloride (TCEP-HCl, ACBR) in PBS, pH = 7.4, then reacted with 2500 equivalents (calculated on the basis of antibody monomers, each containing a single cysteine residue) of Ellman's reagent (DTNB; Sigma Aldrich). The antibody-Ellman's reagent conjugates were purified over an HiPrep 26/10 desalting column (GE Healthcare) running in PBS, pH 7.4, containing 5% sucrose (Weight/Volume; AppliChem) and 10% N,N-dimethylacetamide (DMA; Acros Organics). Ten equivalents of free thiol DM1 drug (Concortis Biosystems) per antibody monomer were dissolved in a small amount of DMA (typically less than 3% of the antibody solution volume) immediately prior to addition to the solution containing the purified antibody-Ellman's reagent conjugate. The reaction was stopped after 5 minutes or 15 minutes for the antibodies in SIP or IgG format, respectively, by the addition of 500 equivalents (per antibody monomer) of a stock solution of iodoacetamide (Sigma Aldrich), dissolved in water at a concentration of 0.1 mmol/L. The resulting ADC products were purified by FPLC over a HiPrep 26/10 desalting column (GE Healthcare) running in the PBS/sucrose/DMA buffer. The ADCs were then formulated at the desired concentration by centrifugation using Vivaspin devices (GE Healthcare), snap-frozen in liquid nitrogen, and stored at −80°C until further use.

Characterization of ADC products

All ADC products were analyzed by SDS-PAGE (Invitrogen), size exclusion chromatography (Superdex200 10/300GL; GE Healthcare), and protein mass spectrometry. Liquid chromatography-mass spectrometry (LC-MS) was performed on a Micromass Quattro API instrument (ESI-TOF-MS) coupled to a Waters Alliance 2795 HPLC using a MassPREP On-Line Desalting Cartridge 2.1 × 10 mm. Water:acetonitrile, 95:5 (solvent A) and acetonitrile (solvent B), with solvent A containing 0.1% formic acid, were used as the mobile phase at a flow rate of 0.3 mL/min. The gradient was programmed as follows: 95% A (0.5 minute isocratic) to 80% B after 1.5 minutes then isocratic for 1 minute followed by 4 minutes to 95% A and finally isocratic for 6 minutes. The electrospray source of LCT was operated with a capillary voltage of 3.0 kV and a cone voltage of 20 V. Nitrogen was used as the nebulizer and desolvation gas at a total flow of 600 L/h. The binding properties of SIP(F8)-SS-DM1 and IgG(F8)-SS-DM1 were analyzed by surface plasmon resonance (BIAcore 3000 System; GE Healthcare) on an EDA-coated CM5 sensor chip (BIAcore) as previously described (15).

Biodistribution studies

The tumor-targeting properties of ADC products were assessed by quantitative biodistribution analysis as previously described (24). Both SIP(F8)-SS-DM1 and IgG(F8)-DM1 were radioiodinated with ^{125}I (PerkinElmer) and chloramine T (Sigma) and purified on a PD-10 column (GE Healthcare). Immunoreactivity of the labeled proteins was confirmed by affinity chromatography, using the recombinant 11-EDA-12 fragment of fibronectin coupled to CNBr-activated Sepharose (GE Healthcare) as previously described (24). Immunocompetent 129SvEv mice, bearing subcutaneously grafted F9 tumors, were injected into the lateral tail vein at a dose of 5 mg/kg (i.e., 125 μg of ADC per mouse). Groups of mice were sacrificed at different time points (3, 24, and 48 hours) after injection. Organs were excised, weighed, and radioactivity was measured using a Packard Cobra gamma counter. Biodistribution results were expressed as the percentage of injected activity per gram of tissue (%IA/g ± SEM).

Immunofluorescence studies

Immunocompetent 129SvEv mice bearing subcutaneously grafted F9 tumors were injected with a single dose of 5 mg/kg of either SIP(F8)-SS-DM1 or IgG(F8)-SS-DM1 (dose in analogy to the therapy) and sacrificed 24 hours after the injection. Tumors were excised, embedded in OCT medium (Thermo Scientific), and cryostat sections (10 μm) were cut. Slides were stained using the following antibodies: rabbit anti-human IgE (Dako Cytomation), to detect the antibodies in SIP format, rabbit anti-human Fc (Dako Cytomation), to detect the antibodies in IgG format, and rat anti-mouse CD31 (BD Biosciences) to detect endothelial cells. Anti-rabbit IgG-AlexaFluor488 (Molecular Probes by Life Technologies) and anti-rat IgG-AlexaFluor594 (Molecular Probes by Life Technologies) were then used as secondary antibodies for microscopic detection of this *ex vivo* immunostaining.

Therapy studies

When tumors reached an average volume of 100 mm^3 (typically 4 to 6 days after subcutaneous tumor implantation), mice were randomly grouped ($n = 5$) and injected i.v. into the lateral tail vein.

In the therapy study with equal milligram doses, mice were injected for 5 consecutive days with the ADCs, both in IgG and in SIP format, or with vehicle (PBS/sucrose/DMA buffer). The daily dose was 5 mg/kg for both ADCs. In the therapy study with equimolar doses, the daily dose was 5 mg/kg for SIP(F8)-SS-DM1 and 9.3 mg/kg for IgG(F8)-SS-DM1 (Fig. 3). The molecular weights of the two products [drug to antibody ratio (DAR) = 2] are 78,928 Da and 145,972 Da, respectively, corresponding to a 1:1.85 ratio.

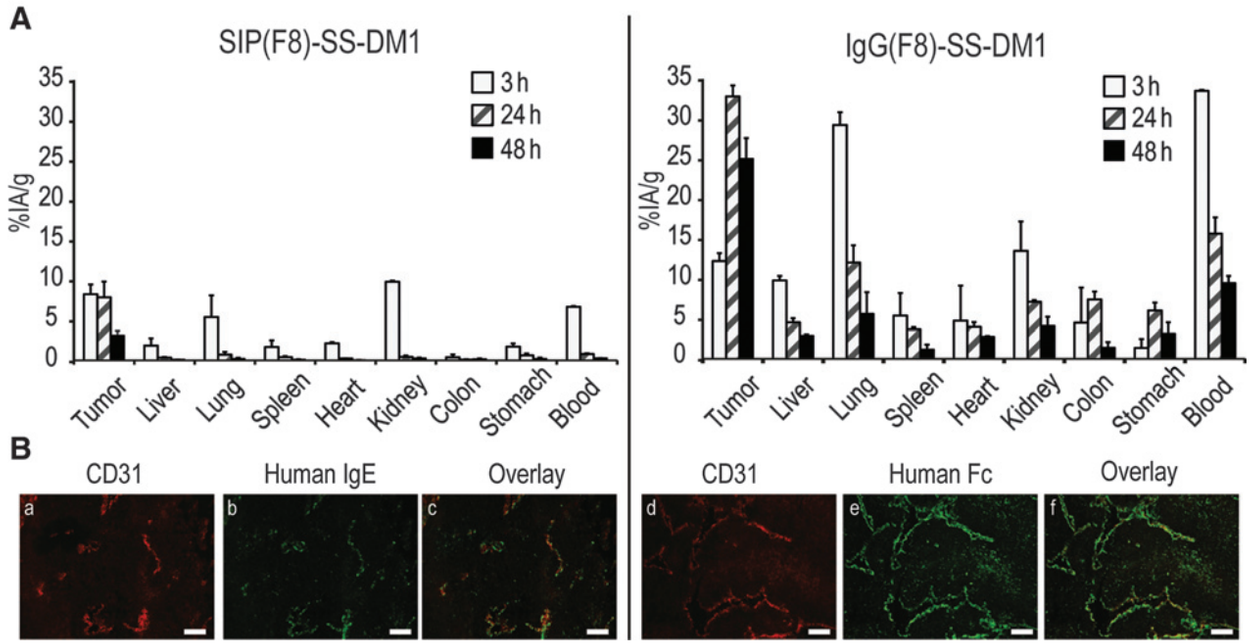

Figure 2.
Biodistribution and immunofluorescence study of SIP(F8)-SS-DM1 and IgG(F8)-SS-DM1. A, biodistribution study of radioiodinated SIP(F8)-SS-DM1 and IgG(F8)-SS-DM1 at 3, 24, and 48 hours after a single intravenous injection (5 mg/kg) into 129 SvEv mice bearing F9 tumors. B, immunofluorescence analysis performed on sections of F9 tumors after a single intravenous injection of SIP(F8)-SS-DM1 (a–c) and IgG(F8)-SS-DM1 (d–f). The antibody localization on tumor blood vessels was revealed by staining in green with anti-human IgE antibodies (b and e), whereas the vascular staining in red was provided by anti-CD31 antibodies (a and d). An overlay of red and green fluorescence is shown in c and f. Scale bar, 100 μm.

Linker stability assay

ADCs were incubated at a concentration of 150 μg/mL in mouse serum (Invitrogen) at 37°C in a shaking incubator. At various time points, aliquots were purified by affinity chromatography onto an antigen-coated resin, based on 11-EDA-12 coupled to CNBr-activated Sepharose (GE Healthcare), washed with PBS and then eluted with 0.1 mol/L glycine solution (pH = 3), prior to analysis by SDS-PAGE and MS. In the case of SIP(F8)-SS-DM1, the relative concentration of ADC was assessed by ESI-MS using SIP(F8) coupled to iodoacetamide as internal standard. For IgG(F8)-SS-DM1, the relative ratios of MS peak intensity for the unmodified and the drug-modified light chain were used for the quantification of drug release rates (Fig. 4).

Results

ADC preparation and characterization

The F8 antibody in SIP and IgG format was coupled to the DM1-SH drug in a site-specific manner, using a recently published procedure (Fig. 1A; refs. 15, 17, 23). While the SIP format contains a single accessible C-terminal disulfide bond for chemical modification, the IgG contains a number of accessible disulfides that can yield a heterogeneous mixture of products. To generate chemically defined IgG-based ADCs, all the hinge region cysteine residues of the IgG heavy chain had to be mutated into serines to allow the selective coupling at the C-terminal cysteine residue of each light chain (Fig. 1A). Both SIP(F8)-SS-DM1 and IgG(F8)-SS-DM1 had a drug-antibody ratio of 2 with excellent purity, as documented by SDS-PAGE, gel filtration, and mass spectrometric analysis (Fig. 1B).

Tumor-targeting studies

The tumor-targeting properties of SIP(F8)-SS-DM1 and IgG(F8)-SS-DM1 were assessed by quantitative biodistribution analysis using radioiodinated protein preparations. Immunocompetent mice bearing murine F9 teratocarcinomas (25) were injected with 125 μg of radioiodinated ADC products, which allowed the measurement of the percent injected activity per gram (%IA/g) in tumor, normal organs, and blood at various time points (3, 24, and 48 hours) after the intravenous administration, in line with previous observations reported for unmodified antibody preparations (26, 27). Figure 2A shows that the IgG-based product displayed a higher absolute uptake in the tumor at later time points compared with its SIP counterpart. However, the tumor: organ ratios for SIP(F8)-SS-DM1 were higher than the ones of the IgG product, and the %IA/g values in the tumor were similar at early time points (8% and 12% at 3 hours, respectively; see also Supplementary Table S1).

An *ex vivo* microscopic analysis of the ADC uptake in the neoplastic lesions confirmed that both SIP(F8)-SS-DM1 and IgG(F8)-SS-DM1 preferentially localize in the subendothelial extracellular matrix, surrounding tumor blood vessels (Fig. 2B).

Therapy studies

In order to compare the therapeutic performance of SIP(F8)-SS-DM1 and IgG(F8)-SS-DM1, which have a molecular weight of approximately 80 kDa and 150 kDa, two studies were performed in F9 tumor–bearing mice: one at equal milligram doses of ADC products and one in which equimolar quantities were administered. The superior therapeutic activity of SIP(F8)-SS-DM1

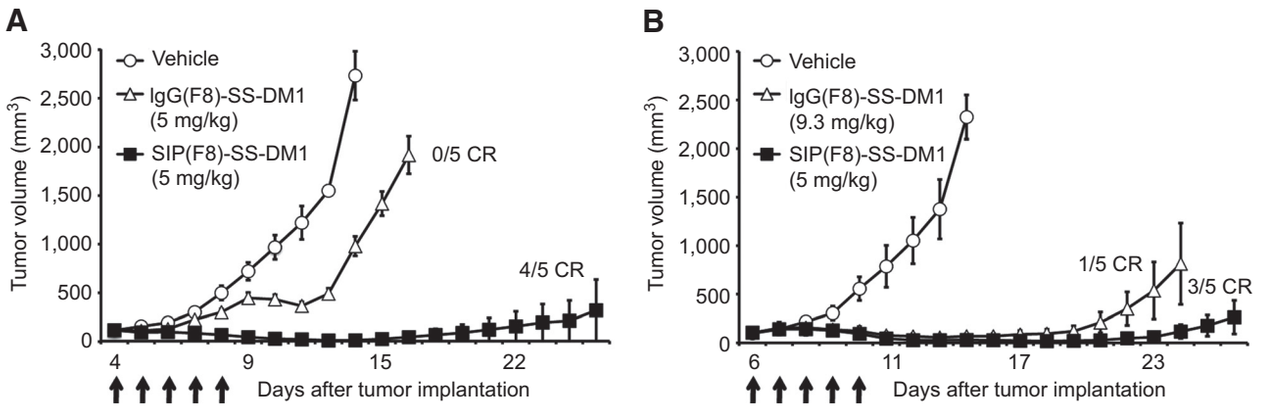

Figure 3.
Therapeutic activity of SIP(F8)-SS-DM1 and IgG(F8)-SS-DM1 against F9 teratocarcinoma. ADCs were used at equimilligram doses (A) or equimolar doses (B). When tumors reached an average of 100 mm^3 of volume, mice were randomly grouped and intravenously injected during 5 consecutive days (arrows) with the vehicle (○), IgG(F8)-SS-DM1 (△) at 5 and 9.3 mg/kg, or SIP(F8)-SS-DM1 (■) at 5 mg/kg. Data represent mean tumor volume (±SEM), $n = 5$ mice per group.

compared with SIP-based ADCs of irrelevant specificity in the mouse has previously been documented (17).

Figure 3A presents a plot of the tumor volume versus time for groups of mice ($n = 5$) treated with saline, SIP(F8)-SS-DM1, or IgG(F8)-SS-DM1 (5 injections at a dose of 5 mg/kg body weight). In this study, the SIP-based ADC product revealed a more potent therapeutic activity ($P < 0.0001$ on day 15), with 4 of 5 mice cured at the end of the experiment.

The body weight of mice was monitored daily. Tumor volumes were measured with a digital caliper (volume = length × width^2 × 0.5). Results were expressed as tumor volume in mm^3 ± SEM. Animals were sacrificed when tumor reached a maximum of 2,000 mm^3 or weight loss exceeded 15%.

When comparing products on an equimolar basis (Fig. 3B), SIP (F8)-SS-DM1 continued to exhibit a superior therapeutic activity ($P < 0.0001$ on day 24), with 3 of 5 mice cured by the SIP product in this experiment.

Stability of the conjugates

In order to investigate the molecular basis for the superior therapeutic activity of SIP(F8)-SS-DM1 compared with its IgG-based counterpart, in spite of the lower uptake values in the tumor (Fig. 2A), we studied the rates of drug release in mouse serum using an MS-based method. The fusion proteins were purified at various time points on an antigen column, followed by MS analysis (Supplementary Figs. S2 and S3). A plot of the percentage of intact ADC conjugate as a function of time reveals that 50% of SIP(F8)-SS-DM1 is cleaved within approximately 3 hours of plasma incubation at 37°C, whereas the half-life of the IgG-based ADC product was >48 hours (Fig. 4). The faster drug release kinetics of SIP(F8)-SS-DM1 may be due to the close spatial proximity of the C-terminal cysteine residues, which, unlike the cysteines in the light chain of IgG-based ADC, can form a disulfide bond upon drug elimination (Fig. 1A and Supplementary Fig. S4). These findings are in keeping with a growing body of data, indicating that site of drug conjugation on the antibody molecule may have substantial impact on therapeutic efficacy and linker stability (28–31).

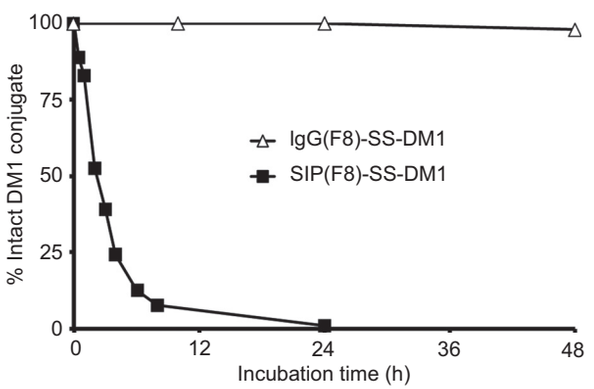

Figure 4.
Kinetics of drug release by ADC incubation in murine plasma. The percentage of intact SIP(F8)-SS-DM1 (■) and IgG(F8)-SS-DM1 (△) products, assessed by ESI-MS analysis after incubation in mice serum, and subsequent purification on antigen resin are plotted as a function of time.

Discussion

We have performed a comparative evaluation of the tumor-targeting properties, release kinetics and anti-cancer performance of two closely related ADCs, based on the F8 antibody in SIP and IgG format. The use of a site-specific drug conjugation method for both formats allowed the preparation of homogenous products and facilitated the analysis of drug release kinetics.

In our study, the ADC product based on the SIP format performed better in therapy experiments than its IgG counterpart, even though the full immunoglobulin exhibited higher tumor uptake values at later time points (i.e., 24 hours after intravenous injection and beyond). Most ADCs in the clinic and in product development are based on the IgG format. While full immunoglobulins have consistently shown better tumor uptake profiles in comparative biodistribution studies (26, 27), suboptimal tumor: organ and tumor:blood ratios, as well as FcRn-mediated continuous recycling processes which deliver ADC products to the endothelium and to the liver, could represent arguments for the experimental investigation of alternative antibody formats. Indeed, Kim and colleagues had previously reported that an anti-CD30 drug conjugate, based on an antibody in diabody format coupled to the anti-tubulin drug monomethyl auristatin

F by a protease-cleavable dipeptide linker, displayed a potent antitumor activity (32).

The dramatic difference in drug release kinetics between SIP and IgG format was unexpected. We had previously reported small differences in the stability of SIP-based ADCs, featuring disulfide-based linkers of different sizes for the F8 antibody in SIP format (33). The faster cleavage of SIP(F8)-SS-DM1 in plasma (compared with its IgG counterpart) is possibly due to the favorable rearrangement of disulfide structures, leading to a stable interchain disulfide bond (Supplementary Fig. S4). This drug release observation is reminiscent of the superior reducing power of 1,4-dithiothreitol (DTT) compared with beta-mercaptoethanol, which is a consequence of DTT's ability to form an intramolecular disulfide bond (34). In the future, it would be attractive to perform quantitative biodistribution studies to assess the stability of the conjugate in blood and other organs, for example by using a newly described dual-radiolabeling strategy, in which drug and mAb moieties incorporate a different radionuclide (35).

The experimental observation that drug release kinetics crucially contributes to therapeutic performance of noninternalizing ADCs suggests that a rapid exposure of cells to high drug concentrations may be more efficacious than a slow release process. This situation is reminiscent of targeted radionuclides for tumor therapy, for which a higher "dose rate" (i.e., the quantity of radiation absorbed per unit of time) results in an increased cytotoxic activity, compared with a radioactive decay (at equal cumulative radiation dose) that takes place over a prolonged period of time (36).

In this work and previous studies, we have focused on tubulin binders and on disulfide bonds as linker–payloads (17, 23, 33). In principle, other linker–payload combinations could be considered. For example, emerging evidence suggests that some proteases (e.g., Cathepsin B), which were originally believed to mediate drug release processes for internalizing ADC products, are also present in the extracellular tumoral environment (37–39) and could potentially be exploited for the release of drugs from noninternalizing ADCs. While many authors consider internalization an absolute requirement for ADC development, increasing experimental evidence gained with ADCs (13, 17, 40), with small molecule–drug conjugates (41), and with polymer–drug conjugates (42) suggests that drugs can be efficiently released in the extracellular tumor environment.

Although it is conceivable that SIP(F8)-SS-DM1 may represent a starting point for the development of more efficacious ADC products, the promising anticancer activity reported in this study and in previous articles (17) may warrant clinical investigations in its own right. The target antigen (i.e., the alternatively spliced EDA domain of fibronectin) is highly conserved across species, facilitating the translation from preclinical studies to clinical studies. Furthermore, ADC therapeutic activity can be potentiated by the action of targeted proinflammatory cytokines (43, 44), with the potential to direct immune recognition at sites of cytotoxic damage. In addition, the vasoactive properties of certain cytokines (principally IL2 and TNF) may be instrumental for the uptake of other therapeutic agents at the tumor site by lowering the interstitial fluid pressure in the tumor environment.

Disclosure of Potential Conflicts of Interest

D. Neri has ownership interest (including patents) in and is a consultant/advisory board member for Philogen. No potential conflicts of interest were disclosed by the other authors.

Authors' Contributions

Conception and design: R. Gébleux, D. Neri
Development of methodology: R. Gébleux, S. Wulhfard, G. Casi, D. Neri
Acquisition of data (provided animals, acquired and managed patients, provided facilities, etc.): R. Gébleux, D. Neri
Analysis and interpretation of data (e.g., statistical analysis, biostatistics, computational analysis): R. Gébleux, D. Neri
Writing, review, and/or revision of the manuscript: R. Gébleux, S. Wulhfard, G. Casi, D. Neri
Administrative, technical, or material support (i.e., reporting or organizing data, constructing databases): D. Neri
Study supervision: D. Neri

Acknowledgments

The authors thank Francesca Pretto, Elena Perrino, and Laura Gualandi for their help with experimental procedures.

Grant Support

The research work was supported by ETH Zürich, Swiss National Science Foundation, Oncosuisse, Federal Commission from Technology and Innovation (KTI, ADC project), Japanese-Swiss Science and Technology Cooperation Program, Maiores Foundation, Philochem AG, SNF (SINERGIA GRANT), and ERC Advanced Grant "ZAUBERKUGEL."

The costs of publication of this article were defrayed in part by the payment of page charges. This article must therefore be hereby marked *advertisement* in accordance with 18 U.S.C. Section 1734 solely to indicate this fact.

Received June 9, 2015; revised August 6, 2015; accepted August 6, 2015; published OnlineFirst August 20, 2015.

References

1. Bosslet K, Straub R, Blumrich M, Czech J, Gerken M, Sperker B, et al. Elucidation of the mechanism enabling tumor selective prodrug monotherapy. Cancer Res 1998;58:1195–201.
2. Krall N, Scheuermann J, Neri D. Small targeted cytotoxics: current state and promises from DNA-encoded chemical libraries. Angew Chem Int Ed Engl 2013;52:1384–402.
3. van der Veldt AAM, Hendrikse NH, Smit EF, Mooijer MPJ, Rijnders AY, Gerritsen WR, et al. Biodistribution and radiation dosimetry of C-11-labelled docetaxel in cancer patients. Eur J Nucl Med Mol Imag 2010;37:1950–8.
4. van der Veldt AAM, Lubberink M, Mathijssen RHJ, Loos WJ, Herder GJM, Greuter HN, et al. Toward prediction of efficacy of chemotherapy: A proof of concept study in lung cancer patients using C-11 docetaxel and positron emission tomography. Clin Cancer Res 2013;19:4163–73.
5. Sievers EL, Senter PD. Antibody-drug conjugates in cancer therapy. In: Caskey CT, editor. Annu Rev Med 2013. p. 15–29.
6. Chari RVJ, Miller ML, Widdison WC. Antibody-drug conjugates: an emerging concept in cancer therapy. Angew Chem Int Ed Engl 2014;53:3796–827.
7. Gerber HP, Senter PD, Grewal IS. Antibody drug-conjugates targeting the tumor vasculature: current and future developments. MAbs 2009;1:247–53.
8. Teicher BA, Chari RVJ. Antibody conjugate therapeutics: challenges and potential. Clin Cancer Res 2011;17:6389–97.
9. Senter PD, Sievers EL. The discovery and development of brentuximab vedotin for use in relapsed Hodgkin lymphoma and systemic anaplastic large cell lymphoma. Nat Biotechnol 2012;30:631–7.
10. Ballantyne A, Dhillon S. Trastuzumab Emtansine: first global approval. Drugs 2013;73:755–65.
11. Mullard A. Maturing antibody-drug conjugate pipeline hits 30. Nat Rev Drug Discov 2013;12:329–33.
12. Bander NH. Antibody-drug conjugate target selection: critical factors. Methods Mol Biol 2013;1045:29–40.

13. Polson AG, Calemine-Fenaux J, Chan P, Chang W, Christensen E, Clark S, et al. Antibody-drug conjugates for the treatment of non-Hodgkin's lymphoma: target and linker-drug selection. Cancer Res 2009;69:2358–64.
14. Neri D, Bicknell R. Tumour vascular targeting. Nat Rev Cancer 2005;5:436–46.
15. Bernardes GJL, Casi G, Truessel S, Hartmann I, Schwager K, Scheuermann J, et al. A traceless vascular-targeting antibody-drug conjugate for cancer therapy. Angew Chem Int Ed Engl 2012;51:941–4.
16. Casi G, Neri D. Antibody-drug conjugates: basic concepts, examples and future perspectives. J Control Release 2012;161:422–8.
17. Perrino E, Steiner M, Krall N, Bernardes GJ, Pretto F, Casi G, et al. Curative properties of noninternalizing antibody-drug conjugates based on maytansinoids. Cancer Res 2014;74:2569–78.
18. Villa A, Trachsel E, Kaspar M, Schliemann C, Sommavilla R, Rybak JN, et al. A high-affinity human monoclonal antibody specific to the alternatively spliced EDA domain of fibronectin efficiently targets tumor neo-vasculature in vivo. Int J Cancer 2008;122:2405–13.
19. Hamblett KJ, Senter PD, Chace DF, Sun MMC, Lenox J, Cerveny CG, et al. Effects of drug loading on the antitumor activity of a monoclonal antibody drug conjugate. Clin Cancer Res 2004;10:7063–70.
20. Lyon RP, Bovee TD, Doronina SO, Burke PJ, Hunter JH, Neff-LaFord HD, et al. Reducing hydrophobicity of homogeneous antibody-drug conjugates improves pharmacokinetics and therapeutic index. Nat Biotechnol 2015;33:733–5.
21. McDonagh CF, Turcott E, Westendorf L, Webster JB, Alley SC, Kim K, et al. Engineered antibody-drug conjugates with defined sites and stoichiometries of drug attachment. Protein Eng Des Sel 2006;19:299–307.
22. Zuberbuhler K, Palumbo A, Bacci C, Giovannoni L, Sommavilla R, Kaspar M, et al. A general method for the selection of high-level scFv and IgG antibody expression by stably transfected mammalian cells. Protein Eng Des Sel 2009;22:169–74.
23. Bernardes GJL, Steiner M, Hartmann I, Neri D, Casi G. Site-specific chemical modification of antibody fragments using traceless cleavable linkers. Nat Protoc 2013;8:2079–89.
24. Pasche N, Woytschak J, Wulhfard S, Villa A, Frey K, Neri D. Cloning and characterization of novel tumor-targeting immunocytokines based on murine IL7. J Biotechnol 2011;154:84–92.
25. Strickland S, Smith KK, Marotti KR. Hormonal induction of differentiation in teratocarcinoma stem cells: generation of parietal endoderm by retinoic acid and dibutyryl cAMP. Cell 1980;21:347–55.
26. Borsi L, Balza E, Bestagno M, Castellani P, Carnemolla B, Biro A, et al. Selective targeting of tumoral vasculature: comparison of different formats of an antibody (L19) to the ED-B domain of fibronectin. Int J Cancer 2002;102:75–85.
27. Wu AM, Senter PD. Arming antibodies: prospects and challenges for immunoconjugates. Nat Biotechnol 2005;23:1137–46.
28. Shen BQ, Xu KY, Liu LN, Raab H, Bhakta S, Kenrick M, et al. Conjugation site modulates the in vivo stability and therapeutic activity of antibody-drug conjugates. Nat Biotechnol 2012;30:184–9.
29. Drake PM, Albers AE, Baker J, Banas S, Barfield RM, Bhat AS, et al. Aldehyde tag coupled with HIPS chemistry enables the production of ADCs conjugated site-specifically to different antibody regions with distinct in vivo efficacy and PK outcomes. Bioconjug Chem 2014;25:1331–41.
30. Tian F, Lu Y, Manibusan A, Sellers A, Tran H, Sun Y, et al. A general approach to site-specific antibody drug conjugates. Proc Natl Acad Sci U S A 2014;111:1766–71.
31. Dorywalska M, Strop P, Melton-Witt JA, Hasa-Moreno A, Farias SE, Galindo Casas M, et al. Effect of attachment site on stability of cleavable antibody drug conjugates. Bioconjug Chem 2015;26:650–9.
32. Kim KM, McDonagh CF, Westendorf L, Brown LL, Sussman D, Feist T, et al. Anti-CD30 diabody-drug conjugates with potent antitumor activity. Mol Cancer Ther 2008;7:2486–97.
33. Steiner M, Hartmann I, Perrino E, Casi G, Brighton S, Jelesarov I, et al. Spacer length shapes drug release and therapeutic efficacy of traceless disulfide-linked ADCs targeting the tumor neovasculature. Chem Sci 2013;4:297–302.
34. Cleland WW. Dithiothreitol, a new protective reagent for SH groups. Biochemistry 1964;3:480–2.
35. Cohen R, Vugts DJ, Visser GWM, Stigter-van Walsum M, Bolijn M, Spiga M, et al. Development of novel ADCs: conjugation of tubulysin analogues to trastuzumab monitored by dual radiolabeling. Cancer Res 2014;74:5700–10.
36. Carlsson J, Eriksson V, Stenerlow B, Lundqvist H. Requirements regarding dose rate and exposure time for killing of tumour cells in beta particle radionuclide therapy. Eur J Nucl Med Mol Imaging 2006;33:1185–95.
37. Warnecke A, Fichtner I, Sass G, Kratz F. Synthesis, cleavage profile, and antitumor efficacy of an albumin-binding prodrug of methotrexate that is cleaved by plasmin and cathepsin B. Arch Pharm 2007;340:389–95.
38. Rothberg JM, Bailey KM, Wojtkowiak JW, Ben-Nun Y, Bogyo M, Weber E, et al. Acid-mediated tumor proteolysis: contribution of cysteine cathepsins. Neoplasia 2013;15:1111–23.
39. Weissleder R, Tung CH, Mahmood U, Bogdanov A Jr. In vivo imaging of tumors with protease-activated near-infrared fluorescent probes. Nat Biotechnol 1999;17:375–8.
40. Ostermann E, Garin-Chesa P, Heider KH, Kalat M, Lamche H, Puri C, et al. Effective immunoconjugate therapy in cancer models targeting a serine protease of tumor fibroblasts. Clin Cancer Res 2008;14:4584–92.
41. Krall N, Pretto F, Decurtins W, Bernardes GJ, Supuran CT, Neri D. A small-molecule drug conjugate for the treatment of carbonic anhydrase IX expressing tumors. Angew Chem Int Ed Engl 2014;53:4231–5.
42. Felber AE, Dufresne MH, Leroux JC. pH-sensitive vesicles, polymeric micelles, and nanospheres prepared with polycarboxylates. Adv Drug Deliv Rev 2012;64:979–92.
43. Gutbrodt KL, Casi G, Neri D. Antibody-based delivery of IL2 and cytotoxics eradicates tumors in immunocompetent mice. Mol Cancer Ther 2014;13:1772–6.
44. List T, Casi G, Neri D. A chemically defined trifunctional antibody-cytokine-drug conjugate with potent antitumor activity. Mol Cancer Ther 2014;13:2641–52.